Magnetic Resonance Imaging 56 (2019) 96–102

Contents lists available at ScienceDirect

Magnetic Resonance Imaging

journal homepage: www.elsevier.com/locate/mri

Original contribution

Overhauser DNP FFC study of block copolymer diluted solution

Bulat Gizatullin*, Carlos Mattea, Siegfried Stapf

Institute of Physics, Ilmenau University of Technology, PO Box 100565, D-98684 Ilmenau, Germany

ARTICLE INFO

Keywords:
NMR
DNP
Block copolymer
Field-cycling
Radical

ABSTRACT

Overhauser dynamic nuclear polarization (DNP) is the dominating hyperpolarization technique to increasing the nuclear magnetic resonance signal in liquids and diluted systems. The enhancement obtained depends on the overall mobility of the radical-carrying molecule but also on its specific interaction with the host molecules. Information about the nature of molecular and radical dynamics can be identified from determining the nuclear T_1 as a function of Larmor frequency by Fast Field Cycling (FFC) relaxometry. In this work, DNP and FFC methods were combined for a detailed study of ^{1}H Overhauser DNP enhancements at 340 mT (X-band) and 73 mT (S-band) for diluted solutions of a block-copolymer with and without the addition of TEMPO radicals. NMR relaxation dispersions of these solutions are measured at thermal polarization and DNP conditions in the X-band, and the obtained DNP data were analyzed by a model of electron-nucleus interactions modulated by translational diffusion. The coupling factors for the two different blocks of the copolymer are obtained independently from DNP and NMRD experiments. An additional contribution from scalar interactions was found for polystyrene blocks.

1. Introduction

The last decade was characterized by a rapid development of hyperpolarization techniques [1–3] in a wide range of applications in NMR mostly for increasing sensitivity. In general, using these techniques provides a hyperpolarized state of nuclei with a significantly improved NMR signal level in comparison with the thermally polarized nuclear system. Of these techniques, dynamic nuclear polarization (DNP), i.e. the transfer of polarization from a quasi-saturated pool of unpaired electrons after microwave irradiation towards nuclei, has been particularly popular and flexible in its application. In the high temperature approximation the enhancement of the NMR signal theoretically amounts to the ratio of the gyromagnetic moments of electrons and nuclei, achieving several thousand for X nuclei and ~660 for ^{1}H [4]. DNP is of significant importance especially for studies of highly diluted solutions [5] as well as for X nuclei with low gyromagnetic ratio and/or low natural abundance.

DNP is frequently subdivided into the well-studied Overhauser effect (OE) [6] and Solid effect (SE) [7]. While SE is mostly observed in solids or highly viscous liquids, and shows a maximum enhancement when the difference of the electron resonance and microwave frequencies is equal to the nuclear Larmor frequency, i.e. $f_e = f_{MW} \pm f_n$ [8], OE in turn is found in low-viscosity liquids and is characterized by a maximum enhancement when the electron spin transitions are saturated by the microwave field, i.e. $f_e = f_{MW}$. At the same time it is required that the electron-nuclear hyperfine interaction is modulated by processes such as translational or rotational diffusion with a rate which is high enough to provide a significant contribution to the spectral density component at the electron Larmor frequency. Assuming the picosecond range of molecular motions typically found in simple liquids [9], the highest enhancement by OE is achieved at relatively low magnetic field strengths, corresponding to, for instance, X- and S-band. However, is has also been shown theoretically and experimentally that OE remains effective even at high fields above 10 T [10], where it is preferably related with fast sub-ps local dynamic. In order to distinguish between different DNP effects the frequency dependence of the enhancement is measured by sweeping the microwave field frequency f_{MW} at a constant polarizing magnetic field or by changing f_e, which can be more readily performed by varying the magnetic field during microwave irradiation and keeping the resonance conditions of the microwave resonator unchanged. Typical modern spectroscopy applications either require the high fields of superconducting magnets and corresponding hardware to generate MW at hundreds of GHz [11], or alternatively shuttling [12] between low and high fields and benefitting from the higher DNP coupling at low fields.

The FFC-DNP method [13] is a recently developed technique for obtaining a hyperpolarized state of the nuclei before cycling the magnetic field and thereby obtaining NMR relaxation dispersion (NMRD)

* Corresponding author.
E-mail address: bulat.gizatullin@tu-ilmenau.de (B. Gizatullin).

https://doi.org/10.1016/j.mri.2018.09.005
Received 14 August 2018; Received in revised form 8 September 2018; Accepted 8 September 2018

profiles with improved selectivity and sensitivity, thus countering the problems of intrinsically low signal-to-noise ratio of the FFC method. The first studies were devoted to investigations of the molecular dynamics and electron-nuclear interactions in polymer systems [14], crude oil [15] and simple liquids with additional radicals [16]. A consequential combination with other recently developed strategies that are based on encoding by relaxation times [17] and generating selectivity by separating the different DNP effects within one system [18] are further steps to enhance specificity and data accuracy in NMRD experiments of complex systems. At the same time, the ability to probe frequency-dependent interactions by FFC provides access to improve models about the specific interaction between electron and nuclei as well as details of molecular dynamic in studied systems.

The concept of Fast Field Cycling (FFC) relaxometry [19] is the determination of the frequency-dependent spectral density function from measuring the longitudinal relaxation time, T_1, as a function of magnetic field strength; the range typically accessed is between 10 kHz and several 10 MHz, making it particularly sensitive to molecular reorientations on timescales between 10^{-8} s and 10^{-4} s. The lack of spectral resolution due to low field homogeneity makes the distinction of multiple components on complex systems difficult, these are only accessible by corresponding multi-exponential fitting in either the T_1 or T_2 domain. The additional effect of electron-nuclear interactions on the total nuclear relaxation rates have been studied with a number of systems containing radicals or paramagnetic species [20]. Important other applications of the FFC technique, where slow molecular motion is expected and has been verified, are found in the fields of hydrated protein systems [21] and liquid crystals [22]. In polymer melts, the established approaches for segmental dynamics, i.e. the Rouse model [23] or tube reptation [24], were intensely studied by FFC over decades.

Block copolymers represent a large class of substances with wide commercial applications, yet dynamics studies remain much scarcer than for homopolymers because of the difficulties to study individual moieties in a single molecule separately. At the same time, controlling the chemical composition and block length in copolymers provides a route towards designing material properties different from those of the corresponding homopolymers, frequently avoiding separation on a macroscopic scale but featuring microphase separation in the melt, solution [25,26] or solid [27]. In solution, the surfactant properties of block copolymers are used in foams, oil additives, dispersion agents, etc. The ability of some block copolymers to form micellar-like structures [28] is intensively used in drug delivery systems [29]. Microphase separation and molecular order is a particular field of interest where the individual dynamics of the different blocks needs to be isolated experimentally.

Recently we showed the feasibility of applying FFC-DNP to studies of molecular dynamics and electron-nuclear interaction in concentrated solutions [17] and melts [14] of polymer materials. In this contribution we present a detailed study of OE in a block copolymer solution, consisting of blocks of polystyrene and polybutadiene (SBS), in the presence of radicals. Molecular dynamic of particular blocks was distinguished by measuring T_2-resolved NMRD at thermal polarization and at DNP OE conditions. A model of electron-nuclear interactions modulated by translational diffusion was used to compute the relevant parameters, including the coupling factor which was compared with the values measured directly by DNP in both S- and X-band, allowing verification of the validity of the model used for fitting the NMRD data. The NMRD of pure SBS solutions was analyzed using contributions from Rouse and Lorentzian components to the spectral density function.

2. Experimental section

Samples of block copolymer solutions were prepared from polystyrene-*block*-polybutadiene-*block*-polystyrene (SBS) obtained from Sigma Aldrich with a molecular weight of 140 kDa and 30% of styrene content, rendering macromolecules of average polybutadiene mass of 100 kDa in between two blocks of polystyrene of about 20 kDa each. In order to study the DNP Overhauser effect, 2,2,6,6-Tetramethylpiperidine 1-oxyl (TEMPO, Sigma Aldrich) was used as a radical. The SBS was diluted in deuterated benzene-d_6 (99,9%, Sigma Aldrich) to a polymer concentration of 10 vol% and then stirred on a vortex mixer for 4 h at +40 °C. For DNP measurements, the solvents were first mixed with TEMPO to obtain the final concentration in SBS solution in a range 0.5–420 mM. The polymer solutions were placed into a 3 mm OD tube, which was flame-sealed immediately after filling. All samples were stored at +5 °C and were measured within 1–2 weeks of preparation. EPR spectra as well as the control of radical concentration in the samples were both performed by EPR using a benchtop EPR spectrometer Miniscope 5000 (Magnettech GmbH, Berlin, Germany).

DNP experiments and relaxation dispersion measurements were performed using a FFC relaxometer (Spinmaster FFC2000, Stelar, Mede, Italy) and a home-built DNP console with two probes operating either at S-band [30] or X-band [31] with corresponding microwave frequencies of 2 GHz and 9.5 GHz, respectively. For the purpose of measuring T_1–T_2 correlation maps and T_2 resolved DNP spectra as well as DNP-FFC relaxation measurements on the FFC relaxometer, an optimized protocol was used [13] (Fig. 1). Acquisition consisted of detection of a train of echo peak intensities by a CPMG pulse sequence with 59 μs echo time. Thus two-dimensional data sets of 3072 × 32 points were acquired from T_1–T_2 correlation measurements. The two-dimensional ILT analysis [32] was performed using a set of 32 × 32 logarithmically distributed values of relaxation times in the range of

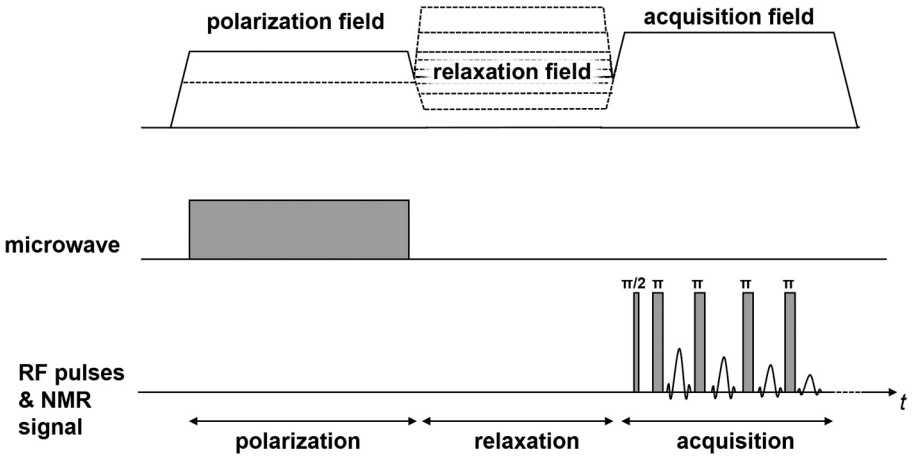

Fig. 1. Pulse sequence for the measurement of T_1 relaxation dispersion profiles using hyperpolarized nuclear spin and T_2 resolving by CPMG sequence.

1–10^4 ms for both T_1 and T_2 values. For the T_2-resolved DNP experiment, the decays obtained by CPMG sequences were fitted by two exponential functions with fixed relaxation times, obtained from the previous experiment, and variable relative amplitude of the corresponding components which are related to the different relaxation rates of ^{1}H nuclei in the corresponding polymer blocks.

Additional values of relaxation times at higher fields were obtained on a SpinSolve benchtop NMR spectrometer operating at 43 MHz (Magritek Ltd., Wellington, New Zealand) and a Bruker Avance III spectrometer at 300 MHz.

3. Theoretical section

3.1. DNP and EPR

In the following, a summary of the derivation of OE enhancement is given to a degree which contains the essential information required for understanding the experimentally accessible factors discussed in this work; for a more fundamental description of the theoretical framework see, e.g., reviews such as [33,34].

The DNP OE enhancement of the NMR signal can be expressed as [33]:

$$E = \frac{P_{DNP}}{P_0} = 1 - \xi f s \frac{\omega_e}{\omega_n}, \tag{1}$$

where P_{DNP} and P_0 are enhanced NMR signal at the DNP condition and the equilibrium thermal polarization, respectively; ω_{e} and ω_{n} are the Larmor frequencies of electron spin and nuclear spin under study. The three factors ξ, f and s are the coupling, leakage and saturation factors usually used to describe OE enhancement. The leakage factor f is given by

$$f(c) = \frac{r_{1,n}^{rad} c}{R_{1,n}}, \tag{2}$$

where $R_{1,\mathrm{n}}$ is the total measure relaxation rate and $r_{1,\mathrm{n}}{}^{\mathrm{rad}}$ is the molar relaxivity due to interactions between electron and nuclear spins, which is multiplied by the radical concentration c. The leakage factor is calculated from NMRD or T_1–T_2 map data, i.e. by using the T_1 values at polarization fields of 73 and 340 mT (S- and X-band) with and without radical.

The saturation factor s is separated into two factors $s_{\mathrm{rel}}(P)$ and $s_{\mathrm{max}}(c)$ which depend on the microwave power and radical concentration, respectively. From the power dependency of the enhancement $E(P)$, the limiting value extrapolated to infinite power enhancement E_{max} can be calculated by [16]:

$$E(P) = 1 - (1 - E_{max}) \frac{P/P_{half}}{1 - P/P_{half}}, \tag{3}$$

where P_{half} is the fitting parameter for which $s_{\mathrm{rel}}(P_{\mathrm{half}}) = 0.5$. The maximum of the DNP saturation factor for a system with three EPR transitions, as is the case for the ^{14}N nitroxide radical with its triplet hyperfine splitting due to the $I = 1$ nuclear spin, is then given by:

$$s_{max}(\omega_{exch}) = \left[3 - 4\left(2 + \frac{\omega_{exch}}{W_e}\right)^{-1}\right], \tag{4}$$

where W_{e} is the longitudinal electron spin lattice relaxation rate and ω_{exch} is the Heisenberg exchange frequency, which depends on the concentration as

$$\omega_{exch} = k_{exch} c, \tag{5}$$

with k_{exch} being the exchange rate that is obtained from the experimentally measured increase of the EPR peak-to-peak linewidth:

$$\Delta B_{pp}(\omega_{exch}) - \Delta B_{pp}(0) = \frac{4}{3} \frac{k_{exch} c}{\sqrt{3}\gamma_e}, \tag{6}$$

The coupling factor ξ is a concentration independent parameter and depends on the type of interaction in the system, magnetic field and temperature.

The final expression for the extrapolated enhancement is given by:

$$E_{max}(c) = 1 - \xi \frac{r_{1,n}^{rad} c}{R_{1,n}(0) + r_{1.n}^{rad} c} \frac{1}{3}\left[3 - 4\left(2 + \frac{\omega_{exch}}{W_e}\right)^{-1}\right] \frac{\omega_e}{\omega_n}, \tag{7}$$

where the remaining fitting parameters are the coupling factor ξ and the ratio ($k_{\mathrm{exch}}/W_{\mathrm{e}}$).

3.2. NMR relaxation dispersion

A model which combines dipolar and contact scalar interactions modulated by translational diffusion [35] was used for the analysis of frequency dependencies of the molar relaxivity $r_{1,\mathrm{n}}{}^{\mathrm{rad}}(\omega)$. The model involves the following correlation time:

$$\tau_t = \frac{2d^2}{D_{\mathrm{n}} + D_e}, \tag{8}$$

where D_{n} and D_{e} are self-diffusion coefficients of the molecules containing nuclear and electron spins, respectively, and d is the minimal distance between electron and nucleus. In case of a high-molecular weight polymer solution, D_{n} is negligibly low in comparison with the diffusion coefficient D_{e} of the TEMPO radical. The important assumption for using this model is the absence of "sticking" conditions where rotational diffusion would dominate the modulation of electron-nucleus interaction. It was shown before that this model can be used successfully for, among others, simple aromatic liquids [16], or in protein solution [36]. The presence of a hydration sphere of paramagnetic centers or additional interaction which leads to an increase of the contribution of rotational diffusion might be taken into account by advanced models [37]. The reduced spectral density for the translational diffusion modulated by dipolar interaction is given by:

$$j_d(u) = \frac{15}{2} u^{-5}\{u^2 - 2 + \exp(-u)\bullet[(u^2 - 2)\sin u + (u^2 + 4u + 2)\cos u]\}, \tag{9}$$

where

$$u = \sqrt{\omega\tau_t/2} \tag{10}$$

The corresponding expression of the reduced spectral density for scalar interaction is:

$$j_s(u) = \frac{1}{2u}[1 + \exp(-u)(\sin u - \cos u)] \tag{11}$$

Consequently the relaxation rates induced by dipolar and scalar interactions might be expressed by [38]:

$$\left(\frac{1}{T_1}\right)_{dip} \propto [j_d(\omega_e - \omega_n, \tau_t) + 3j_d(\omega_n, \tau_t) + 6j_d(\omega_e + \omega_n, \tau_t)] \tag{12}$$

$$\left(\frac{1}{T_1}\right)_{scal} \propto [j_s(\omega_e - \omega_n, \tau_t)] \tag{13}$$

Also it is possible to obtain an expression for the radical induced relaxivity:

$$r_{1,n}^{rad} = \hat{r}^{rad}[M_d(7j_d(\omega_e, \tau_t) + 3j_d(\omega_n, \tau_t)) + (1 - M_d)10j_s(\omega_e, \tau_t)], \tag{14}$$

where $\hat{r}^{rad}$ and $0 < \mathrm{M_d} < 1$ are the amplitude and the relative contribution of dipolar interaction to the total relaxation rate in the limit of $\omega = 0$, respectively. Thus the coupling factor is obtained by using [33]:

$$\xi = \frac{M_d 5j_d(\omega_e, \tau_t) - (1 - M_d)10j_s(\omega_e, \tau_t)}{M_d[7j_d(\omega_e, \tau_t) + 3j_d(\omega_n, \tau_t)] + (1 - M_d)10j_s(\omega_e, \tau_t)} \tag{15}$$

The fitting of NMRD of pure SBS solution without additional TEMPO radical is given by a sum of Rouse [23] and Lorentzian components [38]

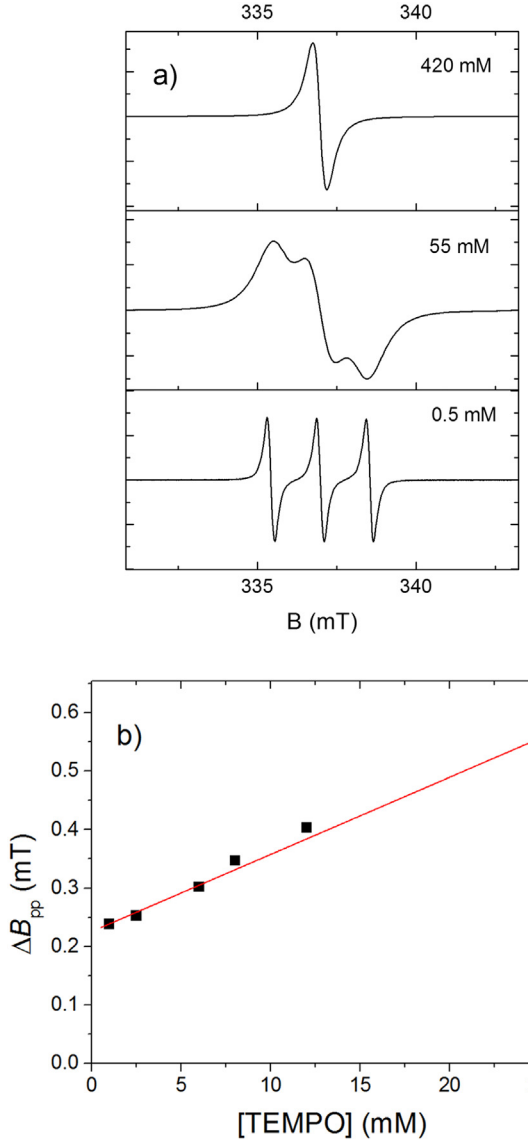

Fig. 2. (a) CW EPR spectra measured for TEMPO in 10 vol% SBS solution in benzene. (b) Concentration dependency of peak-to-peak linear width.

(see discussion below):

$$R_1(\omega_n) = C_L\left(\frac{\tau_L}{1+(\omega_n\,\tau_L)^2} + \frac{4\,\tau_L}{1+(\omega_n\,\tau_L)^2}\right) + C_R\tau_s\;ln\left(\frac{1}{\omega_n\,\tau_s}\right) + C_0, \tag{16}$$

where C_L, C_R and C_0 are prefactors of Lorentzian, Rouse and "Constant" component, τ_L and τ_S are the corresponding correlation times.

4. Results and discussion

4.1. EPR results

In order to obtain the value of the electron spin exchange constant k_{exch}, the concentration dependence of the peak-to-peak linewidth of TEMPO in a 10 vol% SBS solution in benzene were measured for TEMPO concentrations in the range 0.5–25 mM. The obtained widths (see Fig. 2) were fitted by a linear function and the parameter k_{exch} was obtained using (5).

The value of the exchange rate constant is $k_{exch} = (3.1 \pm 0.1)\,s^{-1}\,mM^{-1}$ which is close to the value obtained earlier [16] for a pure benzene solution of TEMPO. This suggests the absence of additional significant line-broadening interactions between TEMPO molecules and the polymer molecule or any of its blocks, which would hint at an additional radical relaxation mechanism.

The linewidth of all three lines is increasing up to concentration c = 55 mM. Above this concentration, the three hyperfine lines of TEMPO begin to overlap, and the linewidth decreases with further increasing radical concentration. As a result, at the highest studied TEMPO concentration c = 420 mM, the EPR spectrum is represented by a single line with a peak-to-peak linewidth of 0.45 mT. Dissolved oxygen in the solution potentially constitutes another source for broadening of the EPR line. However, considering the oxygen effect on EPR and DNP data is beyond the goals of the current study. Nevertheless, the EPR results show that SBS macromolecules in solution have a negligible effect on the EPR properties of the TEMPO radical in benzene solution.

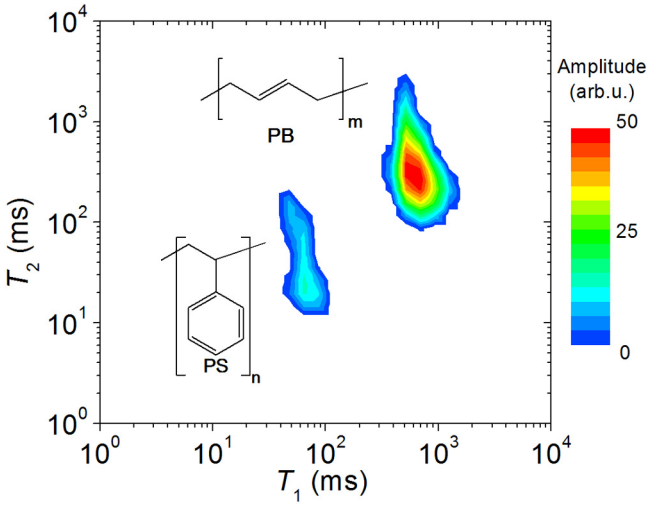

Fig. 3. T_1–T_2 map of SBS in 10 vol% benzene solution at 340 mT magnetic field strength.

4.2. DNP results

A T_2-resolved method for acquiring DNP data was used based on T_2 distribution obtained from the T_1–T_2 correlation map (see Fig. 3) of SBS in solution. Two components clearly distinguished on the T_1–T_2 map at 340 mT magnetic field strength are attributed to the relaxation of different blocks in SBS. In [17] it was shown that the observed peaks with low relative amplitude and mean relaxation times T_1 = 64 ms and T_2 = 35 ms (at 340 mT) correspond to PS blocks. The mean value of relaxation times of corresponding regions were obtained by using logarithmical averaging. The component with values of T_1 = 640 and T_2 = 340 ms and the higher relative amplitude, being proportional to the proton fraction in the PB moieties, corresponds to the PB block and indicates a higher molecular mobility [17]. The values of mean T_2 relaxation time in pure SBS solution and at different concentrations of TEMPO obtained from CPMG decays were used in a biexponential fit to encode and isolate the two components in DNP and FFC measurements.

The T_2-resolved DNP spectra at 7.9 mM TEMPO radical concentration and microwave power of 1 W are presented in Fig. 4. The unequivocal signature of the Overhauser effect for both PS and PB blocks is observed with enhancements of −0.8 and −6.5, respectively. Three peaks corresponding to the hyperfine EPR lines of TEMPO in solution are observed in the DNP spectra. In comparison with more concentrated solutions of SBS [17], the enhancement of the PB blocks signal is higher because OE significantly increases in a system with high molecular mobility such as in a diluted solution. Furthermore, using a nitroxide radical such as TEMPO promotes OE, contrary to the prevailing SE which appears when BDPA is used as a radical in the systems with

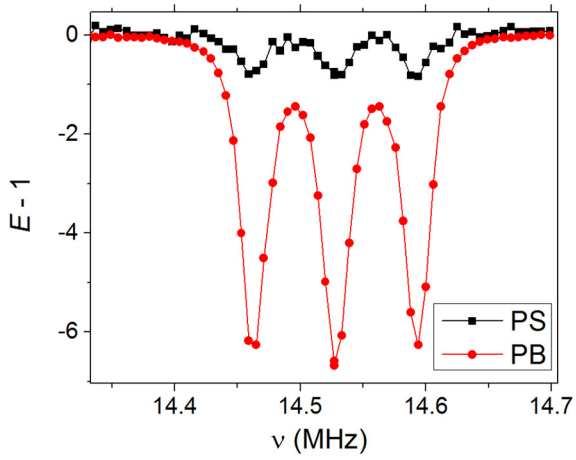

Fig. 4. T_2-separated DNP spectra of the NMR signal enhancement of 10 vol% SBS in C_6D_6 with (7.9 ± 0.6) mM of TEMPO at a MW power of 1 W. Solid lines are guides to the eye.

relatively slow molecular motions [14,18].

The power dependencies of the NMR signal enhancements (Fig. 5) were employed for obtaining the extrapolated value of E_{max}. The extrapolated enhancements $E_{max}(c)$ as a function of TEMPO concentration

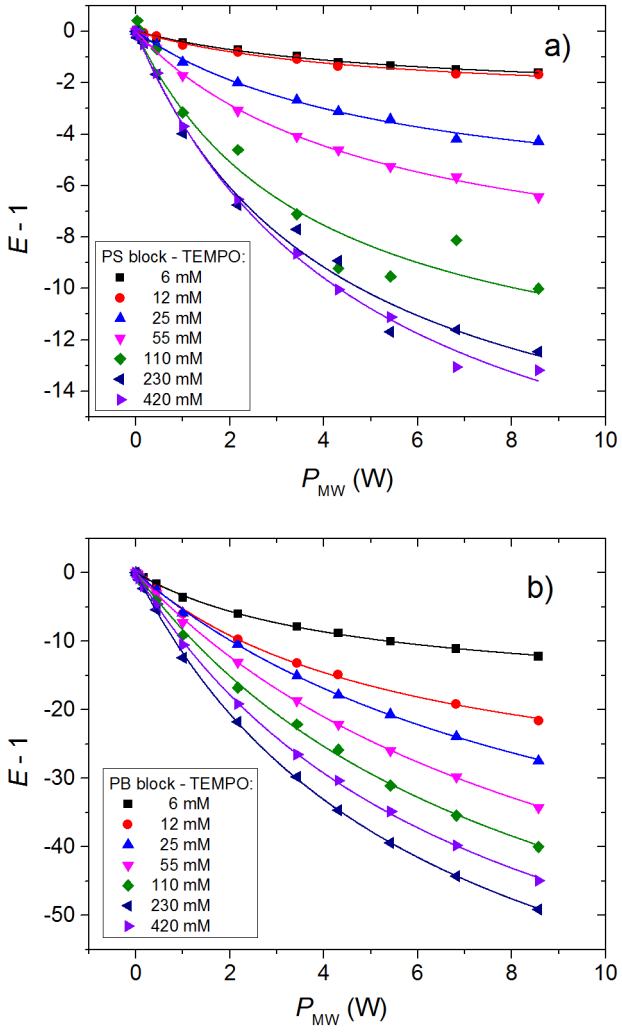

Fig. 5. Power dependencies of DNP enhancement in 10 vol% SBS in C_6D_6 for PS (a) and PB (b) blocks. Solid lines correspond to fitting by Eq. (3).

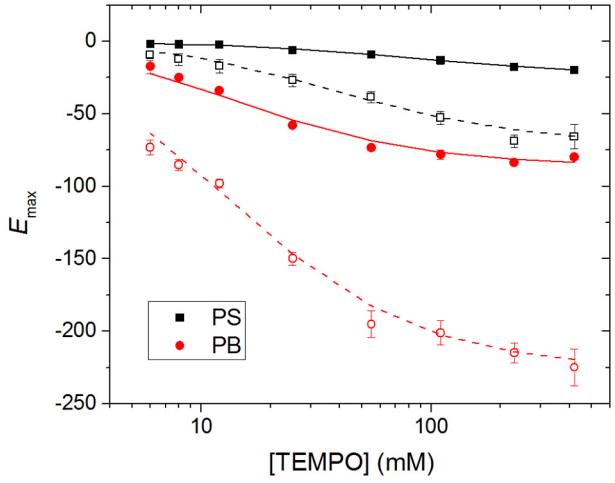

Fig. 6. ^{1}H OE DNP extrapolated maximum enhancement E_{max} of PS and PB blocks at S-band (open symbols) and X-band (solid symbols). The lines represent fits to Eq. (7).

are shown in Fig. 6. Fitting of these curves by Eq. (7) with ξ_{DNP} and k_{exch}/W as fitting parameter is indicated by solid lines. The obtained fitting parameters are presented in Table 1. An increase of the extrapolated enhancement for PB blocks is observed up to 100 mM radical concentration, while above this concentration it depends only on the coupling factor. The coupling factors obtained for PB and PS blocks in solution are 0.335 and 0.108 at S-band and 0.132 and 0.042 at X-band, respectively. The lower coupling and leakage factors for the PS block lead to much lower DNP enhancement values in comparison with the PB block.

The observed values of enhancement in the S-band can significantly decrease experiment time and improve sensitivity in diluted solution. On the other hand, the absolute value of polarization is found to be proportional to the polarization field strength values, which differ by a factor of about 5 for S- and X-band. At the same time the differences between enhancement values for X- and S-band are ~3.7 and 2.5 for PS and PB blocks, respectively. This shows the effectively insignificant advantage of experiments in S-band for this system despite the high value of enhancement. However, it should be noted that no heating effect in excess of 0.1 K/W was observed in S-band measurements up to 10 W in comparison with X-band when active precooling of the sample was used at powers above than 5 W. This is an important advantage of S-band DNP in particular for water solution, dielectric losses of which are much higher than those for benzene.

4.3. NMR relaxation dispersion results

NMRD profiles of different blocks of SBS in benzene solution obtained by T_2-resolved fitting are presented in Fig. 7a. In addition, the dispersion of the radical induced relaxivity is presented in Fig. 7b.

The pure SBS solution NMRD profiles for both polymer blocks (open symbols in Fig. 7a) are characterized by relatively weak dispersions. In accordance with the literature, polymers are expected to follow Rouse dynamics in solutions below the entanglement limit [19,23]. For this reason, Eq. (16) was applied with $C_{lor} = 0$ for the PB block and a satisfactory fit was obtained. At the same time, using only the Rouse model was found to be insufficient for the PS block due to phenyl ring rotation which represents an additional mechanism of relaxation as has been described before in PS melts and solutions [39]. The contribution of the phenyl ring flip with its characteristic rotation time can be considered by an additional Lorentzian component, i.e. $C_{lor} \neq 0$ in (16). The fitted correlation time values corresponding to the models used are summarized in Table 1.

By addition of the TEMPO radical into the solution, the NMRD

Table 1
Fitting parameters from DNP and NMRD experiments obtained by Eqs. (7), (14) and (16).

Block type	PB		PS	
EPR band	S	X	S	X
ξ^{DNP}	0.335 ± 0.01	0.132 ± 0.002	0.108 ± 0.01	0.042 ± 0.005
ξ^{NMRD}	0.328 ± 0.005	0.130 ± 0.008	0.126 ± 0.01	0.040 ± 0.012
$(k_{exch}/W)^{DNP}$ [mM^{-1}]	0.25 ± 0.04	0.31 ± 0.06	0.30 ± 0.05	0.35 ± 0.04
$(k_{exch})^{EPR}$ [$10^6\,s^{-1}\,mM^{-1}$]	3.1 ± 0.1			
M_d	1[a]		0.8 ± 0.05	
τ_t [10^{-9} s] (Diffusion)	0.50 ± 0.8		0.32 ± 0.7	
τ_s [10^{-9} s] (Rouse)	0.25 ± 0.2		0.46 ± 0.1	
τ_L [10^{-9} s] (Lorentzian)	–		2.1 ± 0.3	

[a] M_d was fixed as 1 in PB block case.

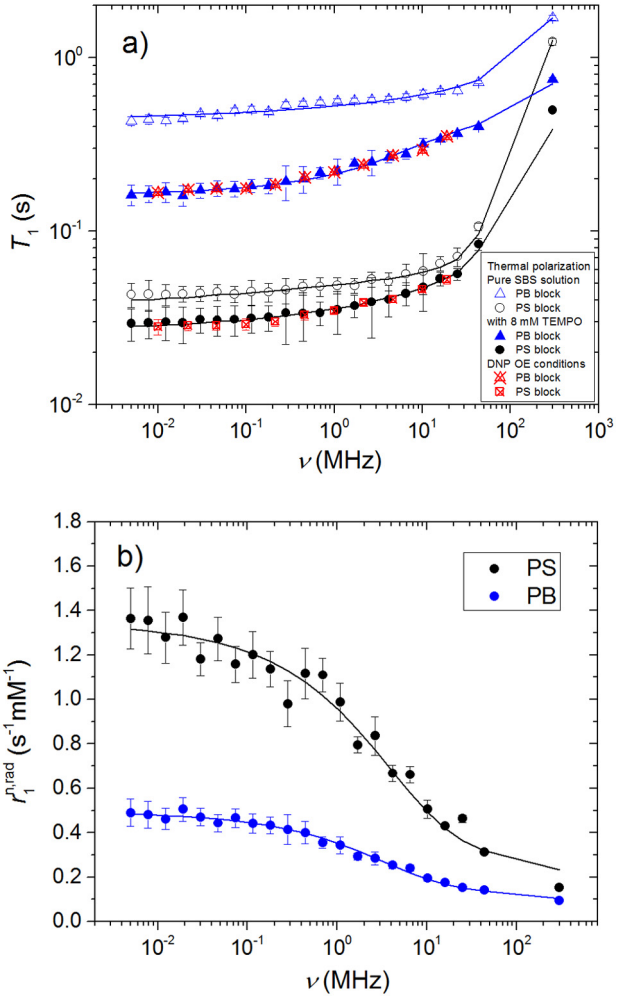

Fig. 7. T_2 resolved relaxation dispersion of spin-lattice relaxation time of PS and PB blocks of SBS in C_6D_6 at 10 vol%. Solid lines are fits to Eq. (16) for pure solution and by sum of bulk and radical induced relaxivity [see Eq. (14)] for solution with radical. (b) Radical-induced (7.9 ± 0.6 mM TEMPO) relaxation rate of PS and PB blocks of the same sample. Solid lines present fitting by Eq. (14).

profiles are noticeably altered (filled symbols in Fig. 7a), this is particularly obvious for the PB block where T_1 values as a whole are reduced significantly and the frequency dependence apparently becomes stronger. Though the effect is somewhat weaker for the PS blocks, T_1 is still shortened almost twofold at low frequencies. Under the assumption – which is supported by the EPR findings – that the addition of TEMPO at small concentration does not change the overall dynamics of the SBS molecule nor the viscosity of the solution, relaxation rates for ^{1}H nuclei can be expressed by additive contributions from the proton dipolar contribution [see Eq. (16)] and the additional relaxivity brought about by the interaction of the ^{1}H with the radical electrons [see Eq. (14)]. The latter relaxivity can then be obtained by subtracting of relaxation rate of pure SBS solution from relaxation rate of SBS solution with TEMPO. This contribution is shown in Fig. 7b: the dispersions of relaxivity for both PB and PS blocks approach a plateau at low fields, whereas the observed decrease with growing field strength traces the spectral density function of dipolar and scalar interaction at the corresponding electron Larmor frequency [20,35].

Fitting of relaxivity dispersion curves according to Eq. (14) with the free parameters r^{rad}, τ_t and M_d are shown in Fig. 7b as solid lines. The coupling factors obtained from calculation of Eq. (15) with parameters obtained from this fit are also reported in Table 1. The solid lines in Fig. 7a corresponding to the SBS solutions with radicals (filled symbols) were obtained by summation of the fitting curves of radical induced relaxivity dispersion curves and fitting curves of the pure SBS solution.

The coupling factors obtained from NMRD and DNP experiments are generally in excellent agreement to each other. However, there possibly remains a higher uncertainty of ξ_{NMRD} of PS because of the influence of the M_d value which is usually defined by few NMRD points at high field. Increasing the number of NMRD values at these field levels can provide improved precision about the scalar interaction contribution. For PB, on the other hand, using this model delivers a reliable fit with fixed $M_d = 1$ which reflects the absence of scalar interaction between PB blocks nuclei and the TEMPO radical. In general, no significant scalar part of interaction is expected for ^{1}H nuclei [9,40,41]. However, the fitting of the relaxation dispersion for the PS protons requires to take scalar interaction into account, and a value of $M_d = (0.8 \pm 0.05)$ shows the best fitting results. For organic solvents with –CH groups in the molecule, TEMPO radical can form hydrogen bonds with solvent molecules which results in an increase of the scalar interaction effect [42]. It can be supposed that it is also possible in the studied system of block copolymer solution. Furthermore, it is reported that aromatic molecules can provide sufficient scalar interaction with the nitroxide radical [16]. The phenyl ring in the PS block is likely to be the source of this sort of interactions. It is also possible that fast rotations of phenyl rings prevail on translational diffusion as mechanism of modulation of electron-nucleus interaction.

The relaxation dispersion curves with enhanced signal at DNP OE condition were obtained for SBS solution with (7.9 ± 0.6) mM TEMPO. It should be noted that no significant difference was observed between NMRD acquired at thermal polarization and at DNP OE conditions. At the given power level of 1 W, using the same time for acquiring data as at thermal polarization conditions allows to decrease the uncertainties of T_1 measurements up to ~5 times for the PB block and ~2 times for PS block while avoiding overheating of the sample.

5. Conclusion

The molecular dynamics parameters and DNP OE coupling factors

were obtained for the individual blocks in polystyrene-polybutadiene-polystyrene block copolymers in deuterated benzene solution both in the pure state and in the presence of TEMPO radical. The Overhauser effect was found as the dominant DNP mechanism in SBS solution with TEMPO for both PS and PB blocks.

The NMR relaxation dispersion curves were successfully described by a model which includes both the dipolar and scalar interactions modulated by translational diffusion. The NMRD of PB blocks show only dipolar interaction between PB chain and TEMPO radicals in solution. The presence of scalar contribution was shown for PS blocks where a contact interaction between TEMPO radical and the phenyl ring is assumed. The corresponding coupling factors for both blocks were calculated.

The good agreement between coupling factors obtained with DNP and NMRD measurements for S- and X-band shows possible application of the used model of electron-nuclear interaction modulated by translational diffusion to simulations of molecular dynamics parameters, which can be used in advanced methods for isolating the actual relaxation dispersion $T_1(\omega)$ of pure substances enhanced by DNP, while at the same time eliminating the additional relaxation contributions of the radical. Studies for applying this concept towards a block-specific or moiety-specific relaxation analysis in complex systems are currently under way.

Acknowledgments

This work was supported by the Deutsche Forschungsgemeinschaft (STA 511/15-1).

References

[1] Atsarkin VA. Dynamic nuclear polarization: yesterday, today, and tomorrow. J Phys Conf Ser 2011;324:012003.
[2] Ardenkjaer-Larsen JH, Fridlund B, Gram A, Hansson G, Hansson L, Lerche MH, et al. Increase in signal-to-noise ratio of > 10,000 times in liquid-state NMR. Proc Natl Acad Sci U S A 2003;100(18):10158–63.
[3] Can TV, Ni QZ, Griffin RG. Mechanisms of dynamic nuclear polarization in insulating solids. J Magn Reson 2015;253:23–35.
[4] Abragam A, Goldman M. Principles of dynamic nuclear polarization. Rep Prog Phys 1978;41:395–467.
[5] Lee JH, Okuno Y, Cavagnero S. Sensitivity enhancement in solution NMR: emerging ideas and new frontiers. J Magn Reson 2014;241:18–31.
[6] Overhauser AW. Polarization of nuclei in metals. Phys Rev 1953;92(2):411–5.
[7] Jeffries CD. Polarization of nuclei by resonance saturation in paramagnetic crystals. Phys Rev 1957;106(1):164–5.
[8] Leblond J, Uebersfeld J, Korringa J. Study of the liquid-state dynamics by means of magnetic resonance and dynamic polarization. Phys Rev A 1971;4(4):1532–9.
[9] Muller-Warmuth W, Meise-Gresch K. Molecular motions and interactions as studied by dynamic nuclear polarization (DNP) in free radical solutions. Adv Magn Opt Reson 1983;11:1–45.
[10] Neugebauer P, Krummenacker JG, Denysenkov VP, Helmling C, Luchinat C, Parigi G, et al. High-field liquid state NMR hyperpolarization: a combined DNP/NMRD approach. Phys Chem Chem Phys 2014;16(35):18781–7.
[11] Leavesley A, Wilson CB, Sherwin M, Han S. Effect of water/glycerol polymorphism on dynamic nuclear polarization. Phys Chem Chem Phys 2018;20(15):9897–903.
[12] Engelke F, Griesinger C. Shuttle DNP spectrometer with a two-center magnet. Phys Chem Chem Phys 2010;12:5830–40.
[13] Neudert O, Mattea C, Stapf S, Reh M, Spiess HW, Münnemann K. Fast-field-cycling relaxometry enhanced by Dynamic Nuclear Polarization. Microporous Mesoporous Mater 2015;205:70–4.
[14] Neudert O, Reh M, Spiess HW, Münnemann K. X-band DNP hyperpolarization of viscous liquids and polymer melts. Macromol Rapid Commun 2015;36(10):885–9.
[15] Ordikhani-Seyedlar A, Neudert O, Stapf S, Mattea C, Kausik R, Freed DE, et al. Evidence of aromaticity-specific maltene NMR relaxation enhancement promoted by semi-immobilized radicals. Energy Fuel 2016;30(5):3886–93.
[16] Neudert O, Mattea C, Spiess HW, Stapf S, Münnemann K. A comparative study of ^{1}H and ^{19}F Overhauser DNP in fluorinated benzenes. Phys Chem Chem Phys 2013;15(47):20717–26.
[17] Gizatullin B, Neudert O, Stapf S, Mattea C. Dynamic nuclear polarization fast field cycling method for the selective study of molecular dynamics in block copolymers. Chemphyschem 2017;18(17):2347–56.
[18] Neudert O, Mattea C, Stapf S. Molecular dynamics-based selectivity for fast-field-cycling relaxometry by Overhauser and solid effect dynamic nuclear polarization. J Magn Reson 2017;276:113–21.
[19] Kimmich R, Anoardo E. Field-cycling NMR relaxometry. Prog Nucl Magn Reson Spectrosc 2004;44(3–4):257–320.
[20] Ravera E, Luchinat C, Parigi G. Basic facts and perspectives of Overhauser DNP NMR. J Magn Reson 2016;264:78–87.
[21] Nusser W, Kimmich R. Protein backbone fluctuations and NMR field-cycling relaxation spectroscopy. J Phys Chem 1990;94(15):5637–9.
[22] Vilfan M, Lahajnar G, Zupančič I, Žumer S, Blinc R, Crawford GP, et al. Dynamics of a nematic liquid crystal constrained by a polymer network: a proton NMR study. J Chem Phys 1995;103(19):8726–33.
[23] Rouse PE. A theory of the linear viscoelastic properties of dilute solutions of coiling polymers. J Chem Phys 1953;21(7):1272–80.
[24] Doi ME, Edwards SF. The theory of polymer dynamics. Oxford: Clarendon Press; 1986.
[25] Nace VM. Nonionic surfactant. polyoxyalkylene block colpolymers. Surfactant science series New York: Marcel Dekker; 1996.
[26] Riess G, Hurtrez G, Bahadur P. Block copolymers. In: Mark HF, Kroschwitz JI, editors. Encyclopedia of polymer science and engineering. New York: Wiley; 1985.
[27] Brereton MG. NMR transverse relaxation function calculated for constrained polymer chains: application to entanglements and networks. Macromolecules 1990;23:1119.
[28] Chiappetta DA, Sosnik A. Poly(ethylene oxide)-poly(propylene oxide) block copolymer micelles as drug delivery agents: improved hydrosolubility, stability and bioavailability of drugs. Eur J Pharm Biopharm 2007;66(3):303–17.
[29] Zeng J, Yang L, Liang Q, Zhang X, Guan H, Xu X, et al. Influence of the drug compatibility with polymer solution on the release kinetics of electrospun fiber formulation. J Control Release Jun. 2005;105(1–2):43–51.
[30] Neudert O, Raich HP, Mattea C, Stapf S, Münnemann K. An Alderman-Grant resonator for S-band dynamic nuclear polarization. J Magn Reson 2014;242:79–85.
[31] Neudert O, Mattea C, Stapf S. A compact X-band resonator for DNP-enhanced fast-field-cycling NMR. J Magn Reson 2016;271:7–14.
[32] Venkataramanan L, Song Y-Q, Hürlimann MD. Solving Fredholm integrals of the first kind with tensor product structure in 2 and 2.5 dimensions. IEEE Trans Signal Process 2002;50(5):1017–26.
[33] Hausser KH, Stehlik D. Dynamic nuclear polarization in liquids. Adv Magn Reson 1968;3:79–139.
[34] Khutsishvili GR. The Overhauser effect and related phenomena. Sov Phys Usp 1960;3:285–319.
[35] Hubbard PS. Theory of electron-nucleus Overhauser effects in liquids containing free radicals. Proc R Soc London, Ser A 1966;291:537–55.
[36] Garcia S, Walton JH, Armstrong B, Han S, McCarthy MJ. L-band Overhauser dynamic nuclear polarization. J Magn Reson 2010;203(1):138–43.
[37] Tóth É, Helm L, Merbach A. Relaxivity of MRI contrast agents. Contrast agents I. 2002. p. 61–101.
[38] Kimmich R. NMR: tomography, diffusometry, relaxometry. Berlin, New York: Springer; 1997.
[39] Cudaj M, Cudaj J, Hofe T, Luy B, Wilhelm M, Guthausen G. Polystyrene solutions: characterization of molecular motional modes by spectrally resolved low- and high-field NMR relaxation. Macromol Chem Phys 2012;213(17):1833–40.
[40] Bennati M, Luchinat C, Parigi G, Turke M-T. Water ^{1}H relaxation dispersion analysis on a nitroxide radical provides information on the maximal signal enhancement in Overhauser dynamic nuclear polarization experiments. Phys Chem Chem Phys 2010;12(22):5737–40.
[41] Sezer D, Prandolini MJ, Prisner TF. Dynamic nuclear polarization coupling factors calculated from molecular dynamics simulations of a nitroxide radical in water. Phys Chem Chem Phys 2009;11(31):6553–4.
[42] Reese M, Turke MT, Tkach I, Parigi G, Luchinat C, Marquardsen T, et al. ^{1}H and ^{13}C dynamic nuclear polarization in aqueous solution with a two-field (0.35 T/14 T) shuttle DNP spectrometer. J Am Chem Soc 2009;131(42):15086–7.